SSC22-WKP2-21

# LunarWSN Node — A Wireless Sensor Network Node Designed for In-Situ lunar Water Ice Detection

Fangzheng Liu
Responsive Environments Group, MIT Media Lab
75 Amherst St, Cambridge, MA, 02139; +1 (617)253-8321
fzliu@mit.edu

Ariel Ekblaw
MIT Space Exploration Initiative, MIT Media Lab
75 Amherst St, Cambridge, MA, 02139; +1 (617) 715-4424
aekblaw@mit.edu

Joseph Paradiso
Responsive Environments Group, MIT Media Lab
75 Amherst St, Cambridge, MA, 02139; +1 (617)253-8321
joep@mit.edu

**ABSTRACT**

In this paper, we present a fully functional cubic sensor node prototype designed to be ballistically deployed from a rover or lander to regions of interest that might be unsafe or impractical for rovers or landers to reach. Unlike helicopters or drones, this system can be deployed in airless environments. Crucially, the nodes are equipped with wireless ranging and wireless communications capabilities, such that each node can be localized by leveraging wireless ranging with triangulation, and a cluster of deployed nodes form an expandable WSN (Wireless Sensor Network), that we term LunarWSN. The hardware redundancy of the network can reduce the chance of failure. Each node is a light (<170g), miniaturized (5cm×5cm×5cm), modular design, that allows sensor payloads to be customized to different scientific missions. As a representative case study, the node described in this paper is equipped with an impedance sensor designed to measure the permittivity of the lunar soil, which infers water content. With the help of LunarWSN, more in situ measurement results can be obtained to acquire meter-scale-resolution knowledge of lunar resource distribution and dynamic phenomena.

## INTRODUCTION

Technologies that enable long-term, wide-range measurements on the lunar surface are crucial for future long-term human presence on the Moon, which is significantly resource-consuming. Water is one the most versatile resources that can serve as drinking water and potential fuel. Ferrying water from the earth is high-cost and unsafe. Taking advantages of local resources is a promising approach that helps to make long-term habitation possible. For now, our knowledge of lunar water deposits is restricted to orbital data and limited surface measurements.[1,2,3] More in situ measurements are essential to detect potential water deposits and confirm the remote sensing information. Moreover, a lot of phenomena of interest are in hard-to-reach areas, such as craters with steep cliffs, caves with poor radio accessibility, rocky piles, etc.[4] These areas are unsafe for current surface exploration systems, such as rovers, which have a risk of wheel damage,[5] and landers. Furthermore, there is increasing demand for more simultaneous data streams from multiple positions across areas of interest. This data is suitable for building models of dynamic phenomena.[4] Unfortunately, to date, rovers can only provide merely a series of single-point measurements. Without mobility, a lander can only investigate areas not far away from itself. The WSN is a technology that can perform long-term measurements in areas of interest and collect simultaneous data from multiple observations, and it is a novel technology for future lunar architecture.[6] Sensor nodes in a WSN can be small, light, low-cost, and easily deployed to hard-to-reach areas. A WSN can reduce the chance of failure through hardware redundancy and expendability, and a set of sensor nodes can cover a large area in a short time with a proper deployment approach.

## BACKGROUND

### *WSN in Planetary Explorations*

The WSN has been long used on earth for environmental monitoring and science inquiry.[7,8,9,10] These examples demonstrate the intrinsic merits of the WSN, which promise huge potential for in situ planetary exploration. The advances of In-Situ sensor technologies will also enhance the science return from future planetary missions.[11] NASA designates Remote Sensing Instruments/Sensors, Observatories and In-Situ Instrument/Sensor as three major research areas within the Sensors and Instruments taxonomy,[11] and the LunarWSN belongs to "Environment Sensors" under the third "In-Situ Instrument/Sensor" category.

A lot of research has been conducted to explore the applications of the WSN in planetary explorations. The PHALANX (NASA Ames Research Center) presents a WSN in which the sensor nodes can be deployed by a cold-gas-propelled projectile launcher.[4] These nodes are designed to expand the exploring capability of the rovers in unsafe areas. The sensor nodes can provide information about various environmental conditions, including volatiles, pressure, temperature, humidity, etc. The nodes can also serve as landmarks, communication relays, and illumination sources for a rover when it is doing subterranean reconnaissance in caves, lava tubes, etc. The ChipSat (Draper Laboratory, Cornell University) is a miniature and lightweight (~5g) spacecraft-on-chip system.[12] Hundreds of ChipSats can be carried by an orbiter. When the orbiter finds a phenomenon of interest from orbit and needs in situ information, it will deploy hundreds of ChipSats to the planetary surface to take ground measurements. The ChipSat uses Commercial-Off-The-Shelf (COTS) sensors such as pressure sensors and magnetometers to study the planetary surface environment. The ChipSat shows a dual exploration architecture that combines remote sensing and in situ explorations. The Lunette (JPL) is a WSN that is composed of miniature landers for in-situ geophysical measurements.[13] Each lander is equipped with a seismometer to collect seismic data for studying the interior of the moon. The landers serve as secondary payloads of an orbital spacecraft, and land on the lunar surface to create a lander network over an area of 10~20km. The Lunar Environment Monitoring Station (LEMS, NASA) is a compact instrument package.[14] With a mass spectrometer and a molecular electronic transducer, a LEMS can measure the lunar exospheric composition. The Space Wireless sensor networks for Planetary Exploration (SWIPE) is another research effort that aims to monitor the planetary surface environment permanently.[15] The sensor nodes in SWIPE are accurately deployed to desired positions through a rover, and the sensor nodes are designed for measuring radiation, temperature, illumination, and dust deposition.

### *In Situ Lunar Water Detection*

The existence of water ice has been proven after decades of lunar exploration.[16] The LCROSS (Lunar Crater Observation and Sensing Satellite, NASA) is a surface measurement for water ice detection and its observations indicate an abundance of ~ 5.6 ± 2.9% by weight (wt.%) of water.[3,17] However, the LCROSS took only a one-point measurement, and more information from ground measurements is essential for placing constraints on the abundance and distribution of water ice. The VIPER (Volatiles Investigating Polar Exploration Rover, NASA) is one of many efforts aimed at determining the distribution and composition of lunar water ice through in situ measurements.[18] The VIPER is a robotic rover equipped with a drill, a neutron spectrometer (NS), a near-infrared (NIR) volatile spectrometer, and a mass spectrometer. The VIPER will analyze the water ice on the surface and subsurface at varying depths and temperature conditions. By measuring the energy of neutrons emitted from the lunar soil, the NS can detect the existence of hydrogen, which implies the presence of water ice.[19] The NIR volatile spectrometer leverages the reflectance spectroscopy of water ice to study its existence.[20]

Another approach can leverage a fundamental property of the lunar soil — dielectric permittivity, which can imply the existence of water ice.[21,22] This has been used in many moisture measurement systems that determine water content in soil or building materials.[23,24] A commercial handheld LCR meter in conjunction with an Electrical Properties Cup (EPC) has been used to measure the impedance spectroscopy of lunar/Martian soil simulants inside the cup.[25] The results show that the impedance is strongly dependent on water content. The Wireless Impedance Sensor Node (WISN) is another research project to study the water content in lunar soil simulant by leveraging its dielectric permittivity.[26] The WISN uses an impedance converter to measure the permittivity of the lunar soil simulant JSC-1A (Johnson Space Center Number One, NASA and the Johnson Space Center) with different water concentrations. The impedance converter feeds a sweeping-frequency (10kHz to 100kHz) AC signal to the lunar soil simulant through a pair of copper probes, which protrude into the simulant. The complex impedance of the simulant at different frequencies can be measured by the impedance converter. The permittivity of the lunar soil simulant can be inferred by leveraging the relationship between the permittivity and the complex impedance.[27] These measurement results showed the dielectric permittivity increases with higher water content.

## OVERVIEW

The LunarWSN is a WSN that is composed of miniature and modular sensor nodes. All sensor nodes can be deployed by a projectile launcher installed on a rover, lander, or dropped by a low-flying satellite. The LunarWSN also permits existing surface exploration systems, such as rovers and landers, to expand their inquiry capability by using massively redundant and expandable hardware. Each LunarWSN sensor node is small and lightweight. The sensor payloads of the sensor nodes can be tailored based on different scientific goals. Our current sensor payload refers to the WISN design and aims to detect the water content in lunar soil by leveraging its dielectric permittivity. After being deployed on the lunar surface, the sensor nodes will localize themselves, set up a communication network, and start the scientific missions.

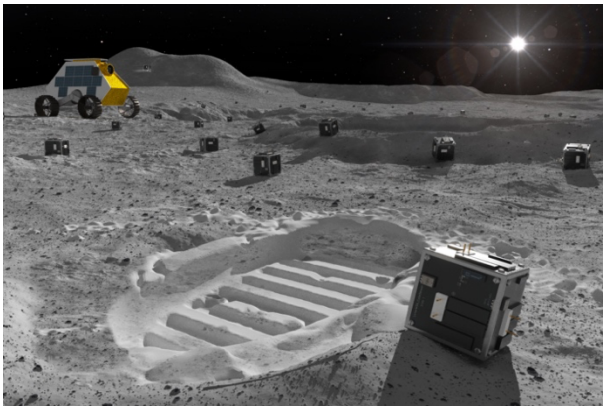

**Figure 1: Artist rendering of LunarWSN working on the lunar surface.**

## LUNAR-WSN DESIGN

### *System Overview*

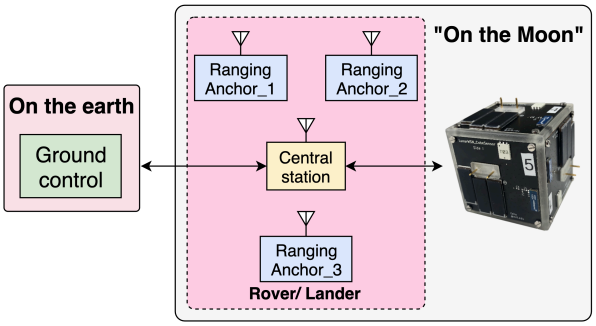


**Figure 2: System block diagram of the LunarWSN**

The whole system diagram is shown as Figure 2. A LunarWSN sensor node localizes itself through wireless ranging with three fixed ranging anchors for 3D positioning. A lunar-based central station keeps a wireless connection with the LunarWSN and relays data back for real-time monitoring and control. We have prototyped one node to represent a node in the LunarWSN. A laptop is used for mission control, and a serial port or network connection between the laptop and a ground station acts as the Earth-Moon link.

### *Shape of The Node*

Different kinds of WSN nodes with various shapes are discussed in prior work. The PHALANX proposed a projectile-like node design with tail fins, however, this design isn't relevant here, since there is no air on the lunar surface. The fins also take excessive space — as much as the projectile body, which holds the sensor payload. We also considered a spherical design; however, most sensor payloads of interest are rarely spherical, which will cause a waste of the node's internal space. Moreover, after touching the lunar surface, a ball-shaped node cannot provide a relatively deterministic landing position and may roll for a long distance, given the low gravity level on the moon. When we want to explore a crater, all spherical nodes may roll down from the cliff and crowd at the bottom. A tetrahedron-shaped node was also considered, based on the SWIPE. This design requires a deterministic landing orientation to guarantee sufficient antenna standoff above the surface for a robust wireless connection. To realize a deterministic landing posture, the nodes need to be put onto the lunar surface in a specific orientation by a rover. This increases the complexity of the mission, and the nodes cannot be deployed to some areas that are unsafe for the rover. To face all the drawbacks mentioned above, we designed a cubic-shaped node, which is shown in Figure 3.

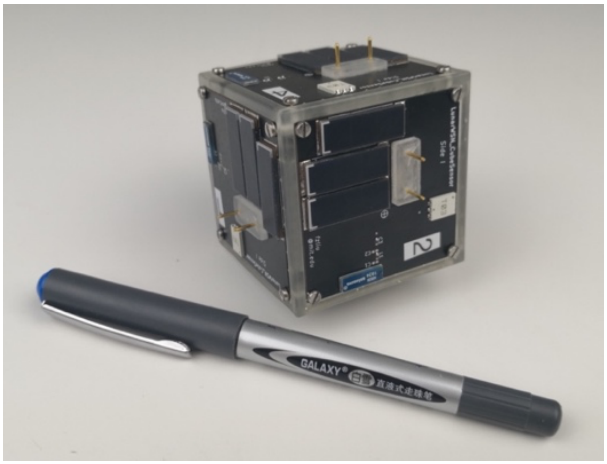

**Figure 3: The cube-shaped node**

The node is a 5cm×5cm×5cm cube. All electronics can fit inside the cubic node, which guarantees an effective usage of the node's internal space. After touching the lunar surface, the cubic shape will stop the node from rolling for too long, and it should halt not far away from the planned location. Other outward-facing components — such as solar panels, chip antennas, etc. — can be easily installed on the flat surfaces of the cube. Since we

don’t know what edges would face upward, downward or towards the sun or towards the lander, lunar base station, or neighboring nodes, the current design features all outward-facing elements on each node face.

### *Node Electronics*

Each sensor node has a PCB (Printed Circuit Board) stack inside. Each board has a specific function and is easily redesigned or replaced.

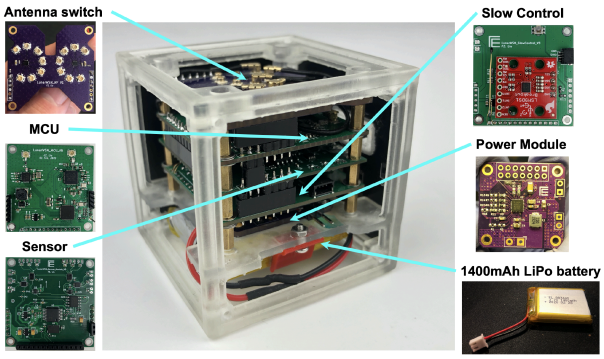


**Figure 4: The structure of the node**

The node is composed of six modules, as shown in Figure 4, and the functions and design of each module are described in Table 1.

**Table 1: sensor node modules function and design**

| Module | Functions | Design |
|---|---|---|
| Antenna switch module | Choosing the antennas which can provide the best radio connection for wireless communication and wireless ranging | Including two SP6T (single pole, six-throw) RF switches (SKY13416-485LF, Skyworks) for both wireless communication and wireless ranging. The RF switches are controlled by the MCU module. |
| Main Control Unit (MCU) module | Performing the wireless communication, wireless ranging, and controls other modules through different interfaces (GPIO, $I^2C$, and SPI). | The main controller IC is a nRF5283 (Nordic). An UWB (Ultra-Wide Band) radio IC (DW1000, decaWave) is used for wireless ranging, and a 2.4GHz IC (nRF24L01+, Nordic) is used to realize wireless communication. |
| Sensor module | Performing main sensing mission. Can be tailored by different mission requirements. | The current sensor module we designed is composed of an impedance convertor IC (AD5933, Analog Devices) and two SP6T circuits. Each SP6T circuit is made up of a SPDT (single pole, double-throw) analog switch (ADG849, Analog Devices) and a SP3T (single pole, three-throw) analog switch (TS5A3359DCUT, Texas Instrument). The SP6T is controlled by the MCU module and selects which node face to use for sensing. |
| SlowControl module | Collecting housekeeping data indicates the node's status, including temperature (through thermistors), battery voltage, landing posture, etc. | Including a four-channel low-power low speed ADC (ADS1115, Texas Instruments), a COTS IMU (Inertial Measurement Unit) module (LSM9DS1 module, Sparkfun). Also including a connector for programming and debugging. |
| Power module & Battery | Harvesting and storing energy. | A MPPT (maximum power point tracker, AD5091, Analog Devices) for energy harvesting, and a 1400mAh LiPo battery. |
| Node face | Six faces on each node. Providing surface for installing antennas, sensor probes, solar panels, and other components that need to be exposed to the external environment. | Each face has a 2.4GHz chip antenna (A5839, Antenova) for wireless communication, an UWB chip antenna (AH086M555003-T, Taiyo Yuden) for wireless ranging, three solar panels (KXOB25_05X3F, ANYSOLAR) for energy harvesting, and a pair of sensor probes for injecting sweeping-frequency AC signal into the MUT (material under test). |

The system diagram is shown in Figure 5.

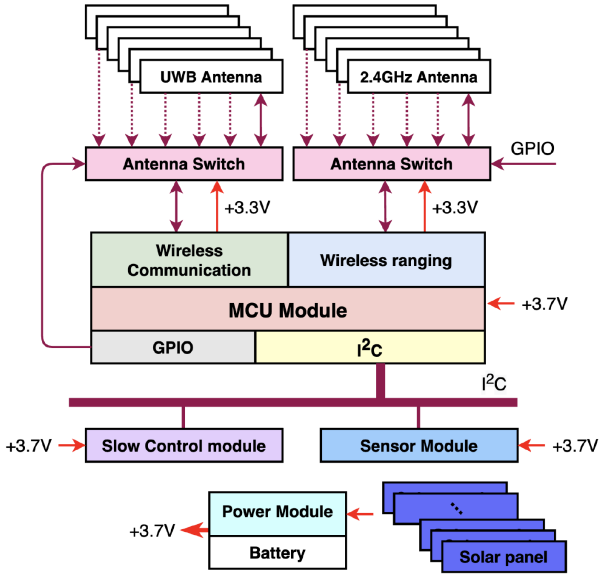


**Figure 5: The node electrical system diagram.**

***Operation Supporting Devices***

We also designed an array of external devices to support the operation of the sensor node. These are three wireless ranging anchors and a wireless communication central station, shown as Figure 6.

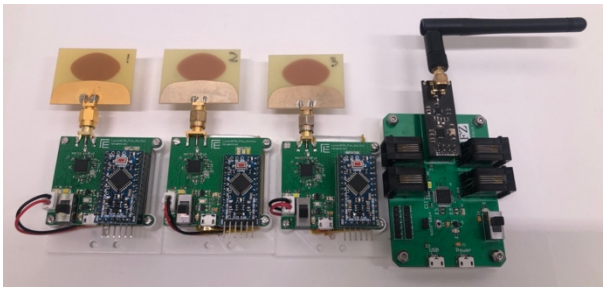

**Figure 6: Three custom ranging anchors and the central station.**

The ranging anchors will be installed at known positions, for example on a rover or lander, and they serve as coordinate references for the node's localization. Each ranging anchor has a DW1000 circuit for wireless ranging, and a COTS Arduino pro mini board. The Arduino board controls the DW1000 circuit and reports the distance measurement to a laptop.

The central station is for relaying data from the node and forwarding commands to the node. The central station has an ATSAMD21G18 (Microchip) circuit for control and a nRF24L01+ module for wireless connection with the sensor node.

## TEST RESULTS

Multiple tests were conducted to validate the performance of the system, including wireless positioning, wireless communication, energy harvesting, and water detection.

***Wireless Positioning***

A wireless positioning test was run for determining the accuracy of the node localization. We leverage wireless ranging and triangulation for localization. The positioning accuracy is largely depended on the accuracy of the distance measurements between the node and each ranging anchor. The distances are measured by using Double-Sided Two-way Ranging (DS-TWR).[29]

In order to measure distance accurately, we need to calibrate the antenna delay. This delay includes the RF propagation time in the antenna, RF switch, and PCB traces. These will introduce significant errors into the distance measurement.

The node was put at some known distances, with one side faced the three ranging anchors. Then the distances were measured between the node face with all three ranging anchors. This process is repeated for each side of the node. 1000 measurements are taken at each distance for each side. The calibration test set-up is shown in **Figure** 7. Each anchor has a GUI for collecting and visualizing data, which is shown in Figure 8.

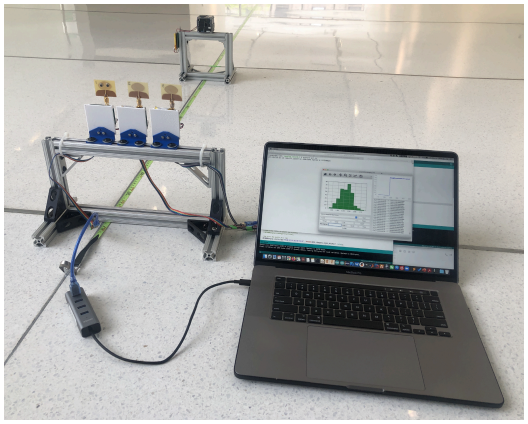

**Figure 7: Antenna delay calibration test set-up.**

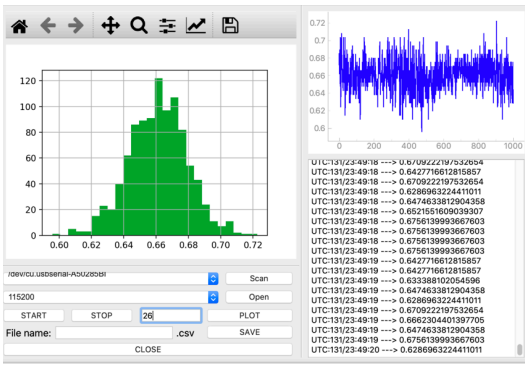


**Figure 8: Antenna delay calibration GUI.**

We use the raw data from one cube face to illustrate the calibration process, and the raw ranging data of one cube face is shown as Figure 9.

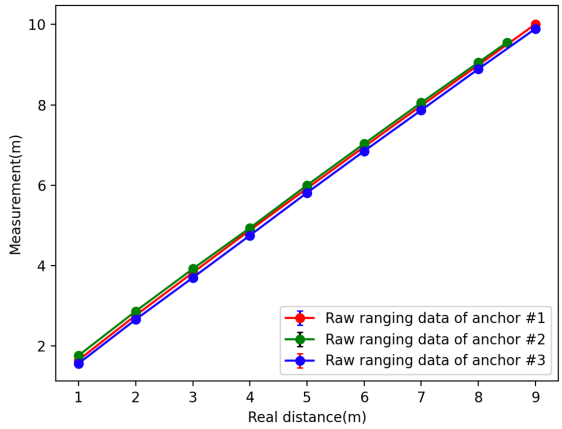


**Figure 9: Ranging test raw data of one side**

To calibrate the antenna delay for each side, we did a function fit for the distance measurements. The least-squares fit is performed for the relationship of each side with each anchor as

$$y(x) = \sum_{m=1}^{M} a_m f_m(x) \qquad (1)$$

$y(x)$ is the distance measurement result. From the raw data plot, the measurements and the real distance show a good linear relationship, so we set the $f_m(x)$ polynomial terms accordingly, i.e., $f_m(x) = x^{m-1}$, and M = 2 (i.e., $y(x) = a_1 + a_2 x$). Then we do the least squares fit by using Singular Value Decomposition (SVD) to get the corresponding coefficients $a_1$ and $a_2$. By doing such a function fit for wireless ranging result, we can lower the ranging errors, shown as Figure 10.

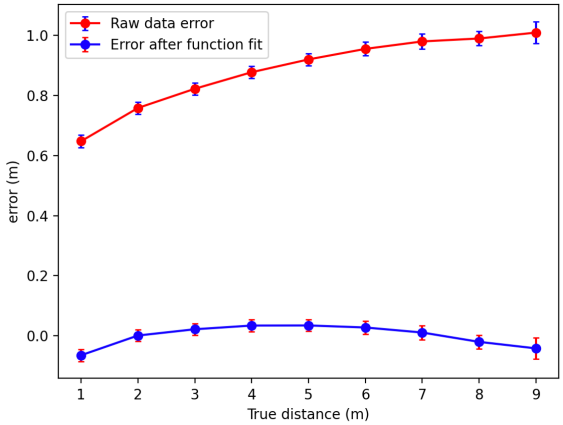


**Figure 10: Wireless ranging error between one side and one ranging anchor, before & after function fit.**

After antenna calibration for each side with each ranging anchor, we set up the localization test in lobby of the MIT Media Lab, since there are grids that are made up of tiles on the floor, and each tile has a deterministic size (4ft × 8ft). The deterministic size of the grids is used as positioning reference. The test environment is shown in Figure 11. The ranging anchors and central station are installed on camera tripods, which are at deterministic positions, as shown in Figure 12. The node is put atop joints of tiles on the floor (which have known positions, as described above) and are readily visible in Figure 13.

**Figure 11: The lobby of MIT Media Lab, used for wireless testing**

**Figure 12: Ranging anchors and central station set up for the localization test.**

**Figure 13: Node is put atop a floor joint**

The sensor node first traverses all the 6 ranging antennas and use the one that can find the most ranging anchors to

localize itself. During the test, the node did wireless ranging with each ranging anchor, and we then use triangulation to get the position of the node. We compared the results with real positions, shown as Figure 14.

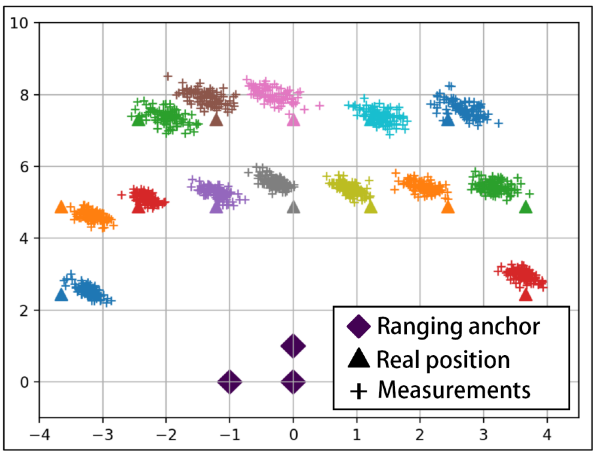


**Figure 14: wireless localization results (meters)**

The test result demonstrated a maximum 0.49m error on the X-axis and a maximum 0.69m error on the Y-axis.

***Wireless Communication***

Communication is another important feature for the node, since keeping RF connection with other nodes or the central station is essential for proper operation for the whole WSN. After deployed on the lunar surface, the sensor node will also traverse all the 6 wireless communication antennas to find the one that can provide a connection with the central station.

We tested the communication range of the node in the large, open lobby of the MIT Media Lab. The node was put at several known distances, with one side facing the central station. The node performed message exchanges with the central station by using the antenna on that side. The station sent a 10-byte-long message to the node, then waited for the reply from the node. After the node receives the message from the central station, it echoes the message back. If the central station didn't receive the echo from the node in 100ms or the message is wrong, the message exchange fails. This message exchange was tested 500 times at each distance for each side of the node. Then the successful exchange percentage is calculated for each side. The test setup and the GUI are shown in Figure 15.

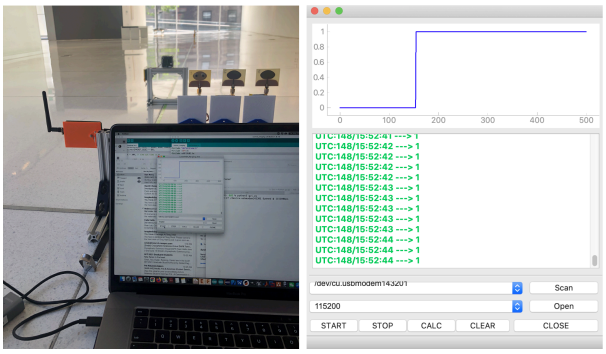


**Figure 15: Communication test setup and GUI**

According to our test results, for successful communication percentage higher than 90%, the maximum communication range of the current node is 7.5m ~ 8.0m.

***Energy Harvesting***

The node can harvest energy through the solar panels on each side to support long-term operations. To test the energy harvesting performance, the node is put under a light irradiance condition that matches the average level expected on the lunar surface. The experimental setup is shown in Figure 16. Only the solar panels on one side are used. A high-power LED simulates overhead sunlight on the lunar surface, where the average daylight solar irradiance is $\sim 1368.0\ W \cdot m^{-2}$.[31] The real irradiance of the LED in the experiment is 170,900 *Lux,* which is $\sim 1350.1\ W \cdot m^{-2}$.

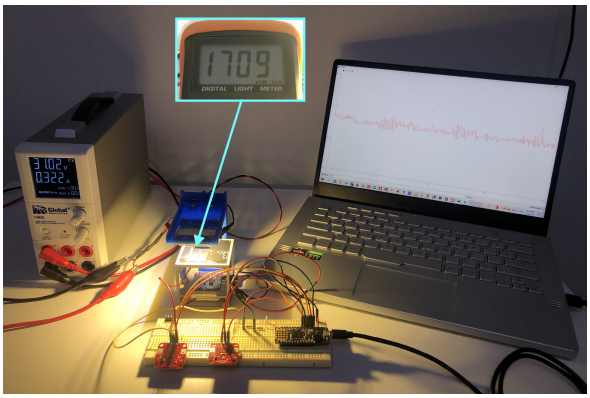


**Figure 16: Energy harvesting test setup**

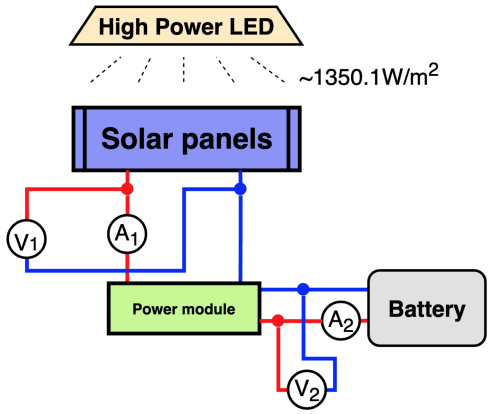


**Figure 17: Energy harvesting test diagram**

As shown in Figure 17, the built-in ADCs of a *Feather M0* board (Adafruit) are used to sample the voltages of the solar panels ($V_1$) and the battery ($V_2$). Two current sensors (INA169, Texas Instrument) are used to measure the current of the solar panels ($A_1$) and battery ($A_2$).

According to our test measurement, the solar power harvested is $P = V_2 * A_2 \approx 18mW$, The power harvesting efficiency $E$, which is the ratio between the power derived by the battery and the power output from the solar panels, i.e., $E = (V_2 * A_2)/(V_1 * A_1)$ is ~83%.

***Water Content Detection***

The water detection performance was tested in a lab environment.

After a sensor node is deployed to the lunar surface, the SlowControl module measures the landing posture by using the acceleration data from the IMU, and find out which side of the node is on the bottom and has contact with the lunar surface. The sensor node will select the sensor probes on this side to do impedance measurement. The water detection sensor is an impedance convertor. It injects a sweeping-frequency AC signal into the MUT through the selected copper probes. In our experiment, we use sand and lunar soil simulant LMS-1 (lunar mare soil simulant,[32] Exolith Lab) with different water content. The response from the MUT is sampled by the built-in ADC of the AD5933, and a DFT (Discrete Fourier transform) is performed by a built-in DSP (Digital Signal Processor). The DSP returns a real (R) and an imaginary (I) data-word. Then the DFT magnitude is

$$Magnitude = \sqrt{R^2 + I^2} \quad (2)$$

To convert the $Magnitude$ to impedance, it must be multiplied by a gain factor.[30] The gain factor at each frequency is scaled by the calibration with a known impedance in contact with the sensor probes. The $Gain\ factor$ at a single frequency is calculated by

$$Gain\ factor = \frac{1}{\frac{impedance_{known}}{Magnitude}} \quad (3)$$

Then the measured impedance ($Z$) at that frequency is given by

$$Z = \frac{1}{Gain\ factor \times Magnitude} \quad (4)$$

We use a 200kΩ resistor for calibration and measured some known resistors; the results are shown in Figure 18.

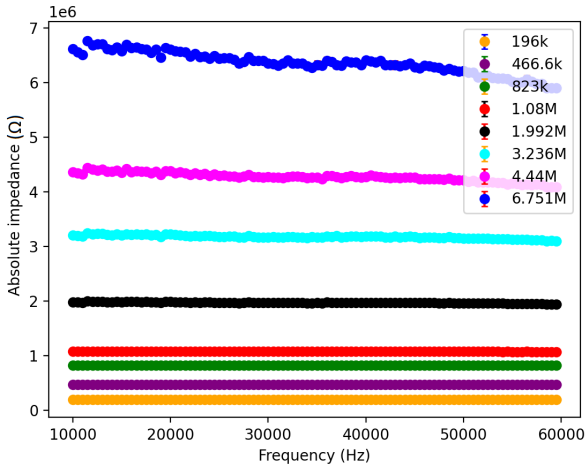


**Figure 18: Responses of resistors after calibration with a 200kΩ resistor.**

The impedance phase $\theta$ is given by

$$\theta = \tan^{-1}(I/R) - \theta_{system} \quad (5)$$

$$\theta_{system} = \tan^{-1}(I_{cali}/R_{cali}) \quad (6)$$

The $I_{cali}$ and $R_{cali}$ are the data-word attained by the calibration with a known resistor. All phase angles need to be corrected instead of dividing the $I$ with $R$ directly.[30] The correction depends on the sign of the $I$ and $R$, as shown in Table 2.

**Table 2: Phase angle correction**

| R | I | Phase angle |
|---|---|---|
| Positive | Positive | $\tan^{-1}(I/R)$ |
| Negative | Positive | $\pi + \tan^{-1}(I/R)$ |
| Negative | Negative | $\pi + \tan^{-1}(I/R)$ |
| Positive | Negative | $2\pi + \tan^{-1}(I/R)$ |

Then the Real ($Z_R$) and Imaginary part ($Z_I$) of the complex impedance are given by:

$$Z_R = Z \times \cos(\theta) \quad (7)$$

$$Z_I = Z \times \sin(\theta) \quad (8)$$

The Real ($\varepsilon'$) and Imaginary ($\varepsilon''$) part of the MUT permittivity is related with the $Z_R$ and $Z_I$ as[27]

$$\varepsilon' = \frac{-Z_I}{g\omega\varepsilon_0(Z_R^2 + Z_I^2)} \quad (9)$$

$$\varepsilon'' = \frac{Z_R}{g\omega\varepsilon_0(Z_R^2 + Z_I^2)} \quad (10)$$

Where $g$ is a constant related to the geometry of the probes (probe area/probes spacing), $\varepsilon_0$ is the permittivity of free space, and $\omega = 2\pi f$ ($f$ is the frequency in Hz). The $\varepsilon'$ is the parameter that we actually use to infer different water content.

Our water content measurement tests are divided into two phases. Both phases use deionized, ultrapure water (Type *I* water) to control the water content in the MUT. In our experiments, only the sensor probes on one side are used, and the test process and data processing (including calibration) for the others are exactly the same.

*Phase I* — testing the sensor by using natural sands with different water content (namely, Dry, 0.89%, 2.14%wt, 3.47%wt by weight (wt.%)) at room temperature (~24℃). This is just for testing the function of the sensor. The sands are put into a plastic cup. The doped ultrapure water is pipetted into the sand, and the water and sand are mixed together by vigorous hand shaking. The sensor node is put into the cup after sensor calibration and the probes fully penetrate into the sands. The central station is installed on top of the cup to get a good wireless connection. The experiment setup is shown in Figure 19. A custom GUI was designed to collect data and monitor & control the experiment, as shown in Figure 20.

**Figure 19: Water detection test setup with sands.**

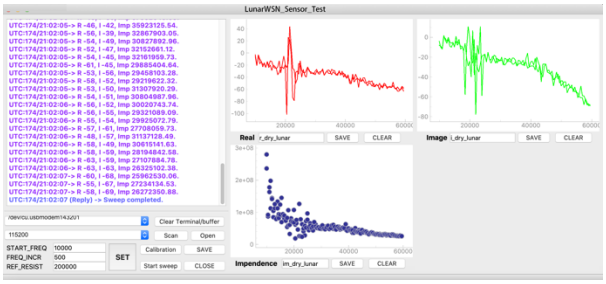


**Figure 20: Water detection test GUI.**

The impedance measurements of the sand with different water content are shown in Figure 21.

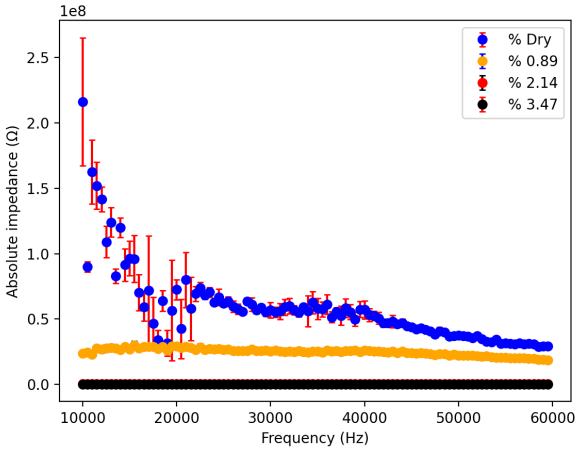


**Figure 21: Water detection test result with sands.**

Phase II — testing the sensor by using LMS-1 lunar mare soil simulant with different water content (Dry, 0.87%, 1.09%, 1.42%, 2.07% by weight (wt.%)) at room temperature (~24°C). The lunar soil simulant is put into a plastic cup, as shown in Figure 22. The doped ultrapure water is pipetted into the simulant. The water and simulant are mixed together by vigorous hand shaking. Every operation is done in a glove box to avoid

contamination. The sensor node is put into the cup after senor calibration, and the probes fully penetrate the soil.

**Figure 22: Water detection test with LMS-1.**

The test results with LMS-1 are shown in Figure 23.

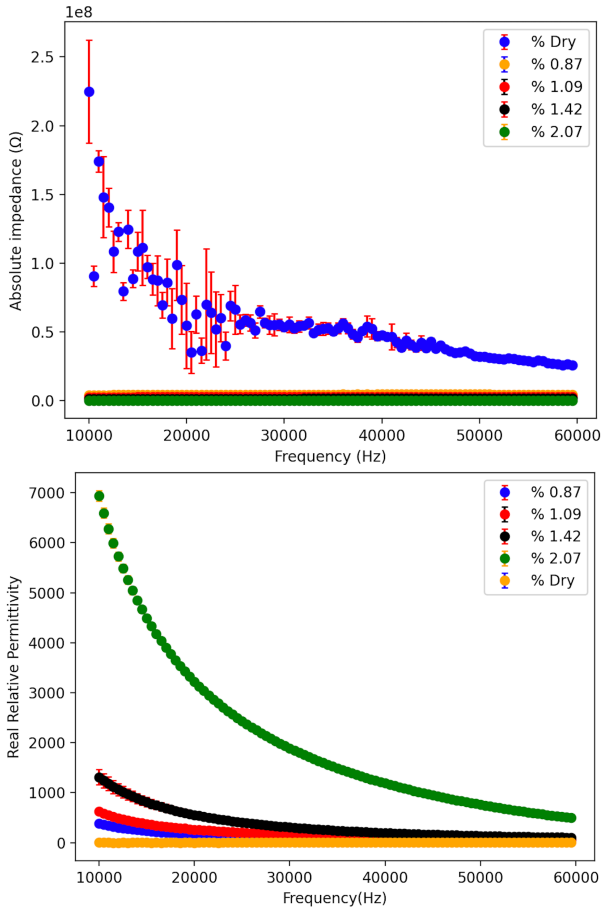


**Figure 23: Water detection test result with LMS-1.**

From the test results, we observed that the absolute impedance drops rapidly with even less than 1% of water added. The real relative permittivity increases more progressively as the water content gets higher.

## DEPLOYMENT APPROACHES

As the sensor node doesn't need specific landing orientation, it can apply different deployment approaches, whether being dropped by a rover to desired positions or ballistically deployed.

### *Compressed Gas Projectile Launcher*

The PHALANX demonstrated a launcher that uses compressed $CO_2$ as propulsive source. The compressed $CO_2$ fills a chamber up to a desired pressure. The $CO_2$ will be released rapidly upon trigger into a barrel and a sensor node is shot out. The sensor node can be deployed up to 30 meters away under the earth gravity level.[4] Compressed $CO_2$ is a good propulsive source, but it is hard to refill on the moon (although enough can be brought along to launch the rover's store of nodes). Of more consequence, the low temperature in some regions of lunar surface will cause a reduced, or unstable vapor pressure of gas, which results in weakened or highly variable thrust. [4]

### *Dropped by A Rover*

Another approach to deploy nodes in different positions is leveraging the mobility of a rover. A set of nodes can be carried by a rover, and each node can be put on the lunar surface when the rover arrives at the desired position. This approach can also guarantee that each node is in a designed orientation on the lunar surface. This is a good choice when the nodes are designed to be deployed in regions of interest that are safe for the rover's movement. However, this approach cannot show the full advantage of the WSN technique in exploring hard-to-reach areas and will use precious rover's operating time.

### *Spring Gun*

A projectile launcher with elastic components, such as springs, is another approach to impart momentum to the sensor nodes. By repeatedly tensioning the spring and shooting the node out, multiple nodes can be deployed. The movement of the nodes will not be affected by air on lunar surface. Therefore, their dropping points would be easily predicted. However, a repeat tensioning mechanism necessitates more power consumption. The springs are also temperature sensitive. Such a projectile launcher has multiple moving parts, which are risky due to the strong vibrations during the launching phase. Here we propose a deployment structure like a gun magazine, shown as Figure 24.

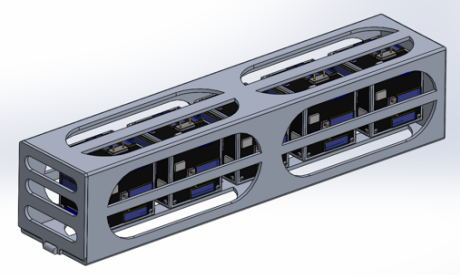

**Figure 24: Sensor node magazine.**

The magazine is loaded with sensor nodes to be deployed. A spring on the inside of the bottom of the magazine

pushes the nodes out one-after-another. The magazine is installed inside a rover, so sensor nodes are sequentially shot to desired locations, as shown in Figure 25.

**Figure 25: LunarWSN nodes deployed from a rover.**

This approach avoids repeatedly tensioning the spring. If the spring is non-linear, the stiffness is not constant. After some nodes are shot out, the spring gets longer, and the force applied to each node will be different. This will cause nonidentical deployment distances. But this kind of error can be estimated. This kind of launcher is simple, low-cost, and robust. For miniature sensor node deployment, this is a very feasible approach. The inside of the magazine needs a careful design, since the surface of the node is not flat due to the protruding sensor probes and other components, hence the magazine needs to avoid sensor nodes being jammed. Another possibility is to stack the magazine atop a dedicated launcher – nodes can be successively inserted into the launcher, which would allow for a longer, more repeatable spring stroke that could launch nodes to much longer range. Of course, when kicking a node strongly from a rover, it must resist toppling in the reduced lunar gravity from large recoil forces.

## DISCUSSIONS + FUTURE WORK

### *Conclusion*

We presented the LunarWSN concept to expand WSNs to space applications. Our design aimed to explore one of the most valuable resources for future lunar missions — water. We showed a miniature (5cm×5cm×5cm) and modular LunarWSN sensor node design and tested its performance in a lab environment. The node uses an off-the-shelf 2.4GHz radio for wireless communication, and the range for a robust wireless communication connection was seen to be 7.5~8m. The wireless positioning tests demonstrated a maximum 0.49m error on the X-axis and a maximum 0.69m error on the Y-axis. The water detection sensor measured the permittivity of the lunar soil simulant with different water content. The results showed that the sensor measurements can detect the differences of lunar soil simulant permittivity and infer the different water content. Our work shows promise for the LunarWSN node to be used in future lunar applications.

### *Future Work*

While we demonstrated basic functions of the sensor node, several improvements need to be made before a deployment would be feasible.

*Positioning* — The current UWB radio used for wireless ranging is very power-consuming (up to ~1$W$). Although the wireless ranging is performed only once, since the node does not have mobility and the position will not change after deployment, the power consumed is still sufficiently large enough to not be ignored. Moreover, in real working cases, the time over which the wireless ranging lasts is uncertain, since the node will try to find all ranging anchors and adjacent nodes within the RF range to get the best positioning performance.[33] This will lead to higher power consumption. During the positioning test, sometimes a node would not find all ranging anchors after it was put on the floor with a random orientation, but all ranging anchors could be found with a small adjustment to the node's orientation. This shows a strong directionality of the node's antenna design, and that the antenna radiation pattern cannot cover all directions. Furthermore, the current design uses chip antennas, whose performance are easily impacted by adjacent components with metal, such as solar panels, screws, and internal PCBs that are on the back of the antennas. To get a better understanding of the RF performance of the node design, high-grade simulations and analysis are essential. The need for anchor nodes may be avoided through other techniques, e.g., successive ranging to a localized rover as it moves. If the deployment process is precise enough, node localization may not be required, as they do not move once they come to rest. Nonetheless, as UWB technology becomes more of a commodity, better ranging performance at lower power can be expected from compact COTS devices.

*Energy harvesting* — Solar energy harvesting is widely-used for space systems. However, for systems operating on the lunar surface, lunar dust will significantly impact the performance of the solar panels, since the lunar dust is extremely adhesive and difficult to get rid of. [34,35] The LunarWSN node will be rolling on the lunar surface after touching down. This could let nearby node get significant dust adhered to their surfaces and significantly reduce the solar panels' performance. Other energy harvesting modalities could be integrated in the sensor nodes – for example, exploiting thermal gradients from the illuminated node sides to the node sides in dark. Power could also be beamed at nodes that are within line

of sight of a steerable-laser remote powering system, such as being proposed in MIT's Lunar Tower.[36] Of course, if the mission lifetime is short enough, sufficient energy to achieve objectives could be pre-stored in the nodes' batteries.

*Wireless communication* — Wireless communication is the most fundamental capability for the node to set up a network for relaying data and commands. The current design is using an off-the-shelf 2.4GHz radio for communication. As reported before, the communication range is very limiting. The communication range needs to be large enough to use less nodes to cover the regions of interest. Wireless sensor nodes are known to be able to work across open spaces with hundreds of meters if not a km of range – better-suited radios can be selected (e.g., LoRaWAN) and the RF antenna and layout in our nodes can be much better optimized to bring this performance into line with what is expected. Of course, nodes can be RF-obstructed by topography on the lunar surface – node deployment will need to take this into account to always provide a reliable connection or multi-hop path back to the Central Station.

*Too much redundancy for a single node* — The current cube-shaped node design has antennas, solar panels, and sensor probes on every side. This guarantees an omnidirectional RF connection, solar-facing orientation, and sensor contact with the lunar surface, hence can improve the robustness of the design. However, this design incurs waste in mass while significantly increasing the node complexity and cost, along with added workload in design, manufacturing, and test phases. A new kind of node design (such as one that always lands or rights into a preferred orientation) can guarantee an omnidirectional RF connection and entail less redundancy at the same time.

*Sensing Configuration* — Although dielectric spectroscopy can indicate water within a few cm of depth and result in other potentially useful geologic measurements, lunar ice may well exist at deeper depths, hence a sensor with more range, such as a Ground Penetrating Radar (GPR),[37] as demonstrated on China's recent Yutu Rover,[38] may be better suited to this mission. A robust, potentially software-based radio system with switchable antennas could be developed to perform GPR, communication, and ranging in a sufficiently compact package. We have also done a preliminary investigation of other sensor payloads that these nodes could host (e.g., radiation, compact geophones, spectroscopy, dust monitoring).[39]

*System ruggedization for lunar mission* — For future lunar missions, the system design should be ruggedized for working in the harsh environment on the lunar surface. Some approaches can be applied, such as using radiation-hardened electronics with coating/isolation, self-monitoring and reset, ESD protections, etc., For good connection with the sensor node, the ranging anchors and central station should be exposed to the outside of a rover/lander. Hence multiple redundancies of ranging anchors and central station hardware are necessary.

## ACKONWLEDGEMENTS

We thank the Responsive Environments group of MIT Media Lab and the Media Lab's Space Exploration Initiative for needed materials and equipment access. We are also very grateful to the resources and support provided by the MIT course "Operating in the Lunar Environment".

### *References*

1. Fisher, E.A., et al., "Evidence for surface water ice in the lunar polar regions using reflectance measurements from the Lunar Orbiter Laser Altimeter and temperature measurements from the Diviner Lunar Radiometer Experiment." Icarus 292, 74–85, 2017.
2. Li, S., et al., "Direct evidence of surface exposed water ice in the lunar polar regions." Proceedings of the National Academy of Sciences, 2018,115 (36) 8907- 8912; DOI: 10.1073/pnas.1802345115
3. Colaprete, A., et al., "Detection of Water in the LCROSS Ejecta Plume." Science 330, 463, 2010, DOI: 10.1126/science.1186986
4. M. Dille, D. Nuch, S. Gupta, S. McCabe, N. Verzic, T. Fong, and U. Wong, "PHALANX: Expendable projectile sensor networks for planetary exploration," IEEE Aerospace Conference, 2020.
5. L. Calle, "Corrosion on mars effects of the mars environment on spacecraft materials," NASA Technical Publication 220238, 2019.
6. NASA, "Technology Horizons: Game-Changing Technologies for the Lunar Architecture." The Tauri Group, 2009. Available online: https://brycetech.com/reports/report-documents/NASA_Technology_Horizons_2009.pdf
7. Mayton, B. et al, "The Networked Sensory Landscape: Capturing and Experiencing Ecological Change Across Scales", *Presence: Teleoperators and Virtual Environments*, 26(2), MIT Press, 2017.
8. K. Pister and J. Kahn and B. Boser, "Smart dust: wireless networks of millimeter-scale sensor

nodes," Highlight Article in Electronics Research Laboratory Research Summary, 1999.

9. J. Manobianco, R.J. Evans, K. Pister, D.M. Manobianco, "GEMS: A Revolutionary System for Environmental Monitoring," Proc. Nanotech 04, pp 422 – 425, 2004.
10. M. Y. Hariyawan, et al., "Wireless Sensor Network for Forest Fire Detection," TELKOMNIKA, vol/issue: 11(3), 2013.
11. Miranda, David. "2020 NASA Technology Taxonomy." No. HQ-E-DAA-TN76545. 2020.
12. Joe Shoer, Rick Stoner, Mason Peck, Zac Manchester, Lorraine Weis, Exploration Architecture with Quantum Inertial Gravimetry and In-situ ChipSat Sensors, NIAC Phase I Final Report, April 28, 2015.
13. John Elliott, Leon Alkalai, A Discovery-class Lunette mission concept for a lunar geopyhysical network, 61st International Astronautical Congress 2010, Prague, Czech Republic, September 27 - October 1, 2010.
14. Malespin, C. A., M. Benna, E. Raaen, M. Sarantos, N. C. Schmerr, L. Dai, and Z. Zhao. "LEMS: Lunar Environment Monitoring Station." In 50th Annual Lunar and Planetary Science Conference, no. 2132, p. 2369. 2019.
15. P. Rodrigues et al., Space Wireless Sensor Networks for planetary exploration: Node and network architectures, 2014 NASA/ESA Conference on Adaptive Hardware and Systems (AHS), Leicester, 2014, pp. 180-187, doi: 10.1109/AHS.2014.6880175.
16. "LunaH-Map Science," Available online: https://lunahmap.asu.edu/science.
17. Schultz, P.H. et al., 2010. "The LCROSS cratering experiment," Science 330 (6003), 468–472.
18. "VIPER Mission Overview," NASA, 2020. https://www.nasa.gov/viper/overview\#KeyFacts
19. "Water on the moon", Available online: https://whyfiles.org/060moons/ourmoon2.html
20. Dobrea, Eldar Noe et al. "The Lunar Infrared Laser Spectrometer For Ice Prospecting And Cave Exploration." (2020).
21. D. Wobschall, "A Theory of the Complex Dielectric Permittivity of Soil Containing Water: The Semidisperse Model," in IEEE Transactions on Geoscience Electronics, vol. 15, no. 1, pp. 49-58, Jan. 1977, doi: 10.1109/TGE.1977.294513.
22. Kremer F, "Dielectric spectroscopy: Yesterday, today and tomorrow," Journal of Non-Crystalline Solids, 305, 1–9 (2000).
23. Wang, James R., and Thomas J. Schmugge. "An empirical model for the complex dielectric permittivity of soils as a function of water content." IEEE Transactions on Geoscience and Remote Sensing 4 (1980): 288-295.
24. Sahu, Riya, Manoj Kumar Gupta, Ranjan Chaturvedi, Sandhya Singh Tripaliya, and Asokan Pappu. "Moisture resistant stones waste based polymer composites with enhanced dielectric constant and flexural strength." Composites Part B: Engineering 182 (2020): 107656.
25. M. G. Buehler et al., "Electrical properties cup (EPC) for characterizing water content of martian and lunar soils," 2006 IEEE Aerospace Conference, Big Sky, MT, 2006, pp. 18 pp.-, doi: 10.1109/AERO.2006.1655752.
26. J. P. Pabari, et al, "Development of Impedance-Based Miniaturized Wireless Water Ice Sensor for Future Planetary Applications," in IEEE Transactions on Instrumentation and Measurement, vol. 61, no. 2, pp. 521-529, Feb. 2012, doi: 10.1109/TIM.2011.2164292.
27. Suresh Seshadri, et al, "Using Electrical Impedance Spectroscopy to Detect Water in Planetary Regoliths," Astrobiology. 781-792. Aug 2008.
28. J.P. Pabari, Y.B. Acharya, U.B. Desai, S.N. Merchant, "Concept of wireless sensor network for future in-situ exploration of lunar ice using wireless impedance sensor," Advances in Space Research, Volume 52, Issue 2, 2013.
29. DecaWave, "APS013 Application note: the implementation of two way ranging with the DW1000." Available online: https://www.decawave.com/wp-content/uploads/2018/10/APS013_The-Implementation-of-Two-Way-Ranging-with-the-DW1000_v2.3.pdf. 2019
30. Analog Devices, "AD5933 data sheet", https://www.analog.com/media/en/technical-documentation/data-sheets/AD5933.pdf
31. V. Badescu, "Moon: Prospective Energy and Material Resources," 10.1007/978-3-642-03629-3, 2012.
32. Exolith Lab. "LMS-1 Lunar Mare Simulant Fact Sheet." Available online:: https://cdn.shopify.com/s/files/1/0398/9268/0862/files/lms-1-spec-sheet-Feb2022.pdf?v=1645817480

33. Wu. H, et al., "Real-time localization algorithm for maritime search and rescue wireless sensor network", Int. J. Distrib. Sens. Netw. 2013, 188–192. 2013.

34. Shahmoradi, J., Maxwell, A., Little, S., Bradfield, Q., Bakhtiyarov, S., Roghanchi, P. and Hassanalian, M., "The Effects of Martian and Lunar Dust on Solar Panel Efficiency and a Proposed Solution," In AIAA Scitech 2020 Forum (p. 1550). 2020.

35. Walton, O.R., "Adhesion of lunar dust," 2007.

36. Lordos, George C., Caleb Amy, Becca Browder, Manwei Chan, Charles Dawson, Paula do Vale Pereira, Sydney I. Dolan et al. "Autonomously Deployable Tower Infrastructure for Exploration and Communication in Lunar Permanently Shadowed Regions." In ASCEND 2020, p. 4109. 2020.

37. Richardson, J.A., et al, "Prospecting Buried Resources with Ground-Penetrating Radar," in Proc. of the Lunar Surface Science Workshop, Paper 5134 (2241), 2020.

38. Li, C. et al, "The Moon's farside shallow subsurface structure unveiled by Chang'E-4 Lunar Penetrating Radar, SciAdv 2020;6:eaay6898, Feb. 26, 2020.

39. Liu, F, "LunarWSN: A Wireless Sensor Network for In-Situ Lunar Water Ice Detection," MS Thesis, Massachusetts Institute of Technology, September 2021